



## Separation and storage of hydrogen by steam-iron process: Effect of added metals upon hydrogen release and solid stability

E. Lorente, J.A. Peña, J. Herguido\*

Catalysis, Molecular Separations and Reactor Engineering Group (CREG), Aragón Institute of Engineering Research (I<sup>3</sup>A), University of Zaragoza, 50018 Zaragoza, Spain

### ARTICLE INFO

#### Article history:

Received 30 September 2008

Received in revised form

26 November 2008

Accepted 19 December 2008

Available online 6 January 2009

#### Keywords:

Steam-iron process

Redox reaction

Hydrogen storage

Hydrogen production

Hydrogen purification

Additive metal

### ABSTRACT

During the last decade, the steam-iron process has re-emerged as a possible way to separate and/or storage pure hydrogen through the use of metallic oxides subjected to redox cycles. The most renamed candidate to achieve this goal has traditionally been iron oxide. Nevertheless, the study of its behaviour along repetitive reduction/oxidation stages has shown that the hydrogen storage density diminishes abruptly from the first cycle on.

To cope with this problem, the inclusion of a second metal oxide in the solid structure has been tried. Isothermal experiments of reduction with hydrogen rich flows and oxidation with steam have been carried out with Al, Cr and Ce as second metals, in nominal amounts from 1% to 10 mol% added to the hematite structure, which has been synthesized in laboratory by coprecipitation. Series of up to seven cycles (reductions followed by oxidations in a thermogravimetric system acting as differential reactor for the gas) have shown that to that point, an almost repetitive behaviour can be obtained, recovering the magnetite (Fe<sub>3</sub>O<sub>4</sub>) structure after each oxidation step.

Since the second metal oxide does not intervene in the reduction/oxidation process, the optimum content of second metal for each species has been determined with the aim to keep the highest hydrogen storage density along cycles.

© 2008 Elsevier B.V. All rights reserved.

### 1. Introduction

Hydrogen can be stored and regenerated using a method of cyclic reduction and oxidation of metallic oxides, usually iron oxides, known as the steam-iron process [1,2]. This method – which was initially developed in the late 19th/early 20th century to produce hydrogen rich gas from gasified coal [3] – stands on the premise that hydrogen can be provided cheaply from fossil sources, such as natural gas during the transition period towards a full hydrogen economy [4].

The steam-iron process operates in two periodic stages, the net reaction being the redox of the metal oxide:



(1) In the first stage (forward reaction), a gas mixture containing hydrogen (for instance, natural gas with a high enough hydrogen content, or a stream resulting from natural gas reforming, hydrocarbon or biomass pyrolysis or gasification) is used to reduce the metal oxide. The water produced in this stage should

be eliminated in order to shift the equilibrium reaction of Eq. (1) towards the reduced metal.

(2) In the second stage (backward reaction), the previously reduced metal is re-oxidized with steam, producing pure hydrogen, while the oxide is regenerated to a certain extent. Therefore, this process can provide a feasible and convenient way to produce a hydrogen stream suitable to feed a PEM fuel cell avoiding the risk of anode poisoning by carbon monoxide impurities.

Iron oxides (Fe<sub>2</sub>O<sub>3</sub>, Fe<sub>3</sub>O<sub>4</sub>) have been typically chosen as metal oxides mediators for the storage and production of hydrogen in the steam-iron system, due to their theoretical high redox capacity per mass unity, availability and economic feasibility [5,6]. The theoretical amount of hydrogen stored and supplied through the redox of iron oxide is calculated to be 4.8 wt% of Fe, which corresponds to the complete oxidation of Fe into Fe<sub>3</sub>O<sub>4</sub>. However, it has been demonstrated that when pure iron oxide is used, the process is adversely affected by sintering or aggregation of particles, caused by the cyclic operation of reduction and oxidation steps [7–9]. This implies that the practical value of hydrogen storage will be lower along time.

Therefore, the selection or development of materials with a low sintering tendency and constant high conversion rates (both for reduction and oxidation) would increase the feasibility of hydro-

\* Corresponding author. Tel.: +34 976 762393; fax: +34 976 761879.  
E-mail address: [jhergui@unizar.es](mailto:jhergui@unizar.es) (J. Herguido).

gen storage by the steam-iron process in comparison with other technologies.

Often in the field of catalysis, certain metals or metal oxides are introduced as promoters into the structure of a metal oxide matrix in order to improve their catalytic activity, stability and/or selectivity. In the same way, the use of iron oxides modified with additives in the steam-iron process could lead to essential improvements with respect to the pure iron oxide, such as the decrease of operational temperatures or the enlargement of the oxide lifetime.

Recently, a number of studies have appeared in literature [10–15], regarding the reduction and oxidation features of iron oxides with promoters. The results of these investigations provide valuable information, especially due to the large number of additives (up to 26 different elements) that have been individually tested. Furthermore, the effect of the promoters has been analyzed on the basis of the local structures and electronic state of the metallic species. As a result of these analyses, it has been proposed that the improvement of stability shown by certain additives could be related to the formation of stable compounds, which prevent the aggregation of iron species during the reduction and oxidation reactions [16–18].

However, several features of these studies, regarding the experimental methodology (e.g. working at non-isothermal conditions or using constant percentage of promoter introduced in the iron oxide) and the presentation of results (e.g. no details about activity, stability and hydrogen storing capacity with respect to the total mass of the solids) are not completely conclusive.

Therefore, in the present study, the reduction and oxidation behaviour of iron oxides modified with Al, Cr and Ce oxides (additives that have been proven to prevent the sintering of iron species during the redox reactions [10]) has been analyzed, with special attention to the influence of the amount of additive in the activity and stability of the solids along cycles.

## 2. Experimental

### 2.1. Preparation and characterization of the iron-based oxides

Samples of pure  $\text{Fe}_2\text{O}_3$  and iron oxides with metal additives were synthesized from the corresponding metal nitrates of Fe, Al, Cr and Ce [ $\text{Fe}(\text{NO}_3)_3 \cdot 9\text{H}_2\text{O}$ ,  $\text{Al}(\text{NO}_3)_3 \cdot 9\text{H}_2\text{O}$ ,  $\text{Cr}(\text{NO}_3)_3 \cdot 9\text{H}_2\text{O}$  and  $\text{Ce}(\text{NO}_3)_3 \cdot 6\text{H}_2\text{O}$ ], and citric acid, by means of the citrate method [19].

For each additive (Al, Cr or Ce), different samples were prepared with nominal quantities from 1 to 10 mol% of added metal to all metal atoms. The synthesized samples (Table 1) were named as  $\text{FeM-x}$ , where  $M$  is the metal (Al, Cr or Ce) introduced as an additive oxide to the hematite and  $x$  represents the percentage of  $M$  content in the solid, as indicated above.

**Table 1**  
ICP and BET characterization results.

Oxide sample	Nominal composition	Additive content ICP (mol%)	Surface area BET ( $\text{m}^2 \text{g}^{-1}$ )
FeM-0	$\text{Fe}_2\text{O}_3$	0.0	2.3
FeAl-2	$\text{Fe}_2\text{O}_3 + \text{Al}_2\text{O}_3$	2.3	3.1
FeAl-5		5.4	9.8
FeAl-10		10.5	14.2
FeCr-2	$\text{Fe}_2\text{O}_3 + \text{Cr}_2\text{O}_3$	2.4	3.0
FeCr-5		5.1	3.5
FeCr-10		9.8	2.9
FeCe-1	$\text{Fe}_2\text{O}_3 + \text{CeO}_2$	1.0	5.2
FeCe-3		3.2	4.8
FeCe-6		5.9	6.9
FeCe-7		7.0	–

**Table 2**  
Redox experimental conditions.

Sample mass	20 mg
Particle size	100–160 $\mu\text{m}$
Inlet flow rate	750 mL (STP) $\text{min}^{-1}$
Pressure	1 bar
Temperature	450 °C
Number of cycles	7
Reduction: $\text{H}_2$ partial pressure	0.5 bar
Time on stream	Until complete reduction
Oxidation: $\text{H}_2\text{O}$ partial pressure	0.2 bar
Time on stream	20 min

According to the citrate method, an aqueous solution of citric acid was added to a concentrate solution of the metal nitrates, with equimolecular relation of citric acid to metal cations. The mixture was kept stirred at 80 °C until a gel was formed. The gel product was dried overnight in an oven at 110 °C. After that the material was calcined in air at 700 °C for 6 h.

The characterization of the solids involved: X-ray diffraction (XRD), elemental analysis (ICP), specific surface area (BET) and temperature programmed reduction (TPR-TG).

### 2.2. Redox cycle experiments

The activity tests for the reduction and oxidation of the iron oxide-based samples were performed in a thermobalance (*CI Electronics MK2*) acting as a differential reactor.

A sample mass of 20.0 mg, with a sieve fraction of 100–160  $\mu\text{m}$ , and a total flow rate of 750 mL (STP)  $\text{min}^{-1}$  were used for all the experiments. From previous experiences [20], using different amount of samples and sieve fractions of  $\text{Fe}_2\text{O}_3$ , and varying the total gas flow rate, it could be concluded that with the above conditions there was no bed depth effects or diffusional limitations. All experiments were carried out at 450 °C under atmospheric pressure.

Each redox cycle was made up of four successive steps: reduction, inertization, oxidation, and inertization. During the reduction step, the samples were treated with a 50:50 gas mixture of hydrogen and nitrogen until complete reduction was achieved. The inertization steps (nitrogen flow for 5 min) were essential to remove the remaining reactive gases of the previous step from the system. In the oxidation step, a mixture of steam and nitrogen was fed and the partial pressure of steam, 0.2 bar, was controlled by saturating part of the inert gas flow at a proper temperature. The duration of the oxidation step was fixed to 20 min.

The reduction and oxidation reactions of the studied oxides were repeated in the same conditions (which are summarized in Table 2) for seven cycles, in order to evaluate their stability.

## 3. Results and discussion

### 3.1. Material properties

X-ray diffraction measurements from the different iron-based oxides (Fig. 1) showed the characteristic diffraction peaks due to hematite ( $\text{Fe}_2\text{O}_3$ ). For the sample added with Ce, a separate Ce containing phase ( $\text{CeO}_2$ ) was detected, but any diffraction peaks ascribed to Al and Cr oxides were not observed for the samples containing these additives. These observations suggest low enough content, high dispersion of the additives, formation of non-crystalline compounds or compounds giving the same diffraction peaks as those of  $\text{Fe}_2\text{O}_3$  [10].

The additive contents of the synthesized oxides measured by ICP are given in Table 1 along with the BET specific surface areas of the samples. It can be observed that the incorporation of additives does not lead to a significant increase in the surface areas, compared to

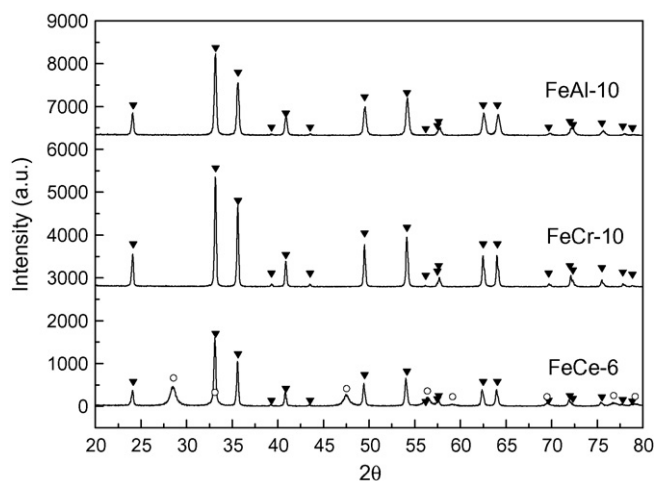


**Fig. 1.** XRD patterns of iron-based oxides with Al, Cr or Ce as additive; (▼)  $\text{Fe}_2\text{O}_3$ ; (○)  $\text{CeO}_2$ .

the pure iron oxide (FeM-0) and only in the case of Al added oxides, higher surface areas were found for increasing Al content. Finally, no correlation could be found between the specific surface area of the solids and their reaction activity.

The characterization of the iron oxides with additives by means of dynamic reduction experiments (temperature programmed reduction) using hydrogen or methane as reducing gases, was performed in the thermogravimetric system.

Fig. 2 shows the weight loss percentage (100% corresponds to the maximum weight loss after complete reduction of each sample), as a function of temperature, obtained from the hydrogen TPR-TG reduction tests. The reduction behaviour of pure  $\text{Fe}_2\text{O}_3$  is also represented for comparison purposes. By examining these results, it can be proven that the reduction of all the samples starts at approximately the same temperature (around 350–400 °C), and to a greater or lesser extent, all graphs show the typical shape, with a shoulder at a degree of reduction of about 11%, which points to the stepwise reaction via  $\text{Fe}_3\text{O}_4$  [21]. On the other hand, as the main difference among the studied oxides, it can be observed that lower reduction rates were registered for increasing percentages of Al and Cr, whereas the amount of Ce did not have a significant effect on the reduction kinetics. These observations must be taken into account when the isothermal redox cycle experiments are performed, since different reduction times will be necessary to completely reduce each oxide.

The behaviour of the iron oxides during dynamic reduction with  $\text{CH}_4$  was also analyzed. The results of these TPR-TG experiments for one sample of each additive are represented in Fig. 3, as well as the one obtained with pure iron oxide, included to allow the comparison. Since the reduction of the samples was not completed at the end of the experiments (800 °C), the weight loss percentages were calculated using the maximum weight loss registered in the hydrogen reduction experiments. All oxides with additives show reduction curves with a similar shape compared to the pure iron oxide. However, the reduction of the iron oxides with additives starts at a higher temperature (around 550 °C) than the pure hematite, which implies that the separation of  $\text{H}_2$  from  $\text{H}_2/\text{CH}_4$  mixtures could be performed at higher temperatures if these materials are used.

### 3.2. Redox behaviour

In order to evaluate the effect of the additive content during reduction–oxidation cycling (seven cycles), series of experiments were carried out in the thermogravimetric system, and the results

obtained for each studied additive (Al, Cr and Ce) are presented in Fig. 4 and discussed below. The weight changes registered during the successive redox cycles ( $\Delta W$ ) are plotted using relative percentage values calculated by dividing the absolute weight change over the maximum weight loss (due to the initial reduction step), which was experimentally proven to be different for each solid. As a consequence, these representations are mainly used to compare the reduction and oxidation rates, as well as the relative regeneration capacity of the oxides, related to the weight lost in the first reduction.

However, in order to compare more properly the behaviour of the iron oxides with different additives, and different amounts of additive for a given metallic pair (e.g. Fe–Al, Fe–Cr, Fe–Ce), the calculation of the “hydrogen storage density” was considered. This

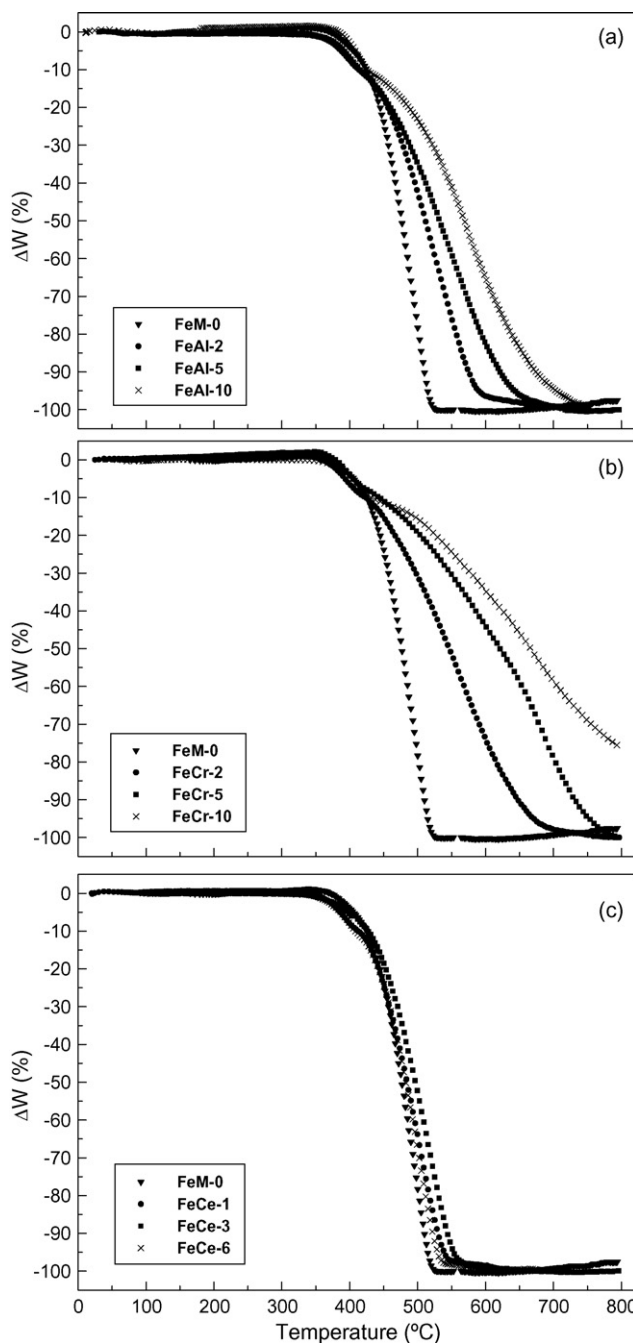


**Fig. 2.**  $\text{H}_2$  TPR-TG profiles of (a) Al, (b) Cr, and (c) Ce added oxides.  $P_{\text{H}_2} = 0.05$  bar,  $\beta = 5^\circ\text{C min}^{-1}$ .

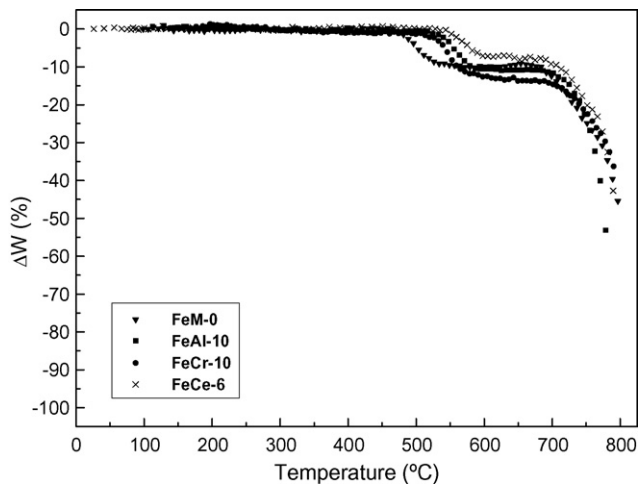


**Fig. 3.** CH<sub>4</sub> TPR-TG profiles of iron-based oxides with different additives.  $P_{\text{CH}_2} = 0.05$  bar,  $\beta = 5^\circ\text{C min}^{-1}$ .

parameter is defined as the ratio of total amount of hydrogen released after each oxidation step to the absolute weight of the reduced solid, and can be easily evaluated from the absolute weight changes registered in the redox experiments, by taking into account

the stoichiometry of the oxidation reaction. In order to make clear the effect of additive amount, the values of hydrogen storage density after the first and seventh cycles are represented in Figs. 5–7 as a function of additive percentage.

The maximum theoretical hydrogen storage density of each solid is also shown in these graphs. To calculate such value, the amount of hydrogen that would be produced during the complete oxidation of Fe to magnetite is considered. It is therefore assumed that the additive does not contribute to the formation of hydrogen (although this fact was not experimentally proven, it would correspond to the worst possible scenario). On the other hand, the amount of additive is taken into account when calculating the theoretical weight of the reduced sample. For that reason, the larger the additive content, the smaller the corresponding hydrogen storage density value.

As a visual reference, Figs. 5–7 include the plots of three lines, denoted hereafter as “theoretical line”, “first cycle line” and “seventh cycle line”. Each of these lines is obtained by connecting the corresponding values of hydrogen storage density (theoretical, after one cycle and finally after seven cycles) for all the solids. The relative position of these lines will give information about the activity and stability of the solids as a function of additive percentage. From a graphical point of view, the objective of introducing additives to the iron oxides would be reflected by the overlap of the “first cycle line” and “seventh cycle line” (stability criterion), in the nearest possible point to the “theoretical line” (activity criterion).

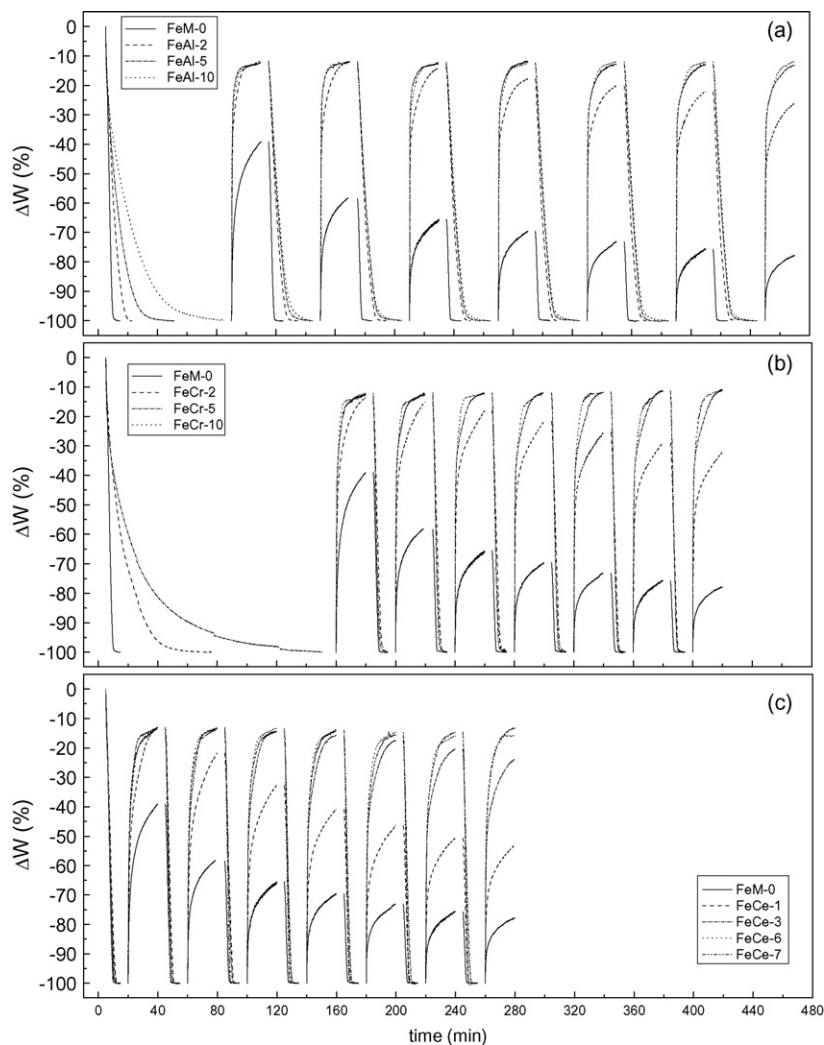


**Fig. 4.** Weight change of (a) Al, (b) Cr, and (c) Ce added oxides during reduction–oxidation cycles at standard experimental conditions (see Table 2 for details). First reduction of FeCr-10 is intentionally left.

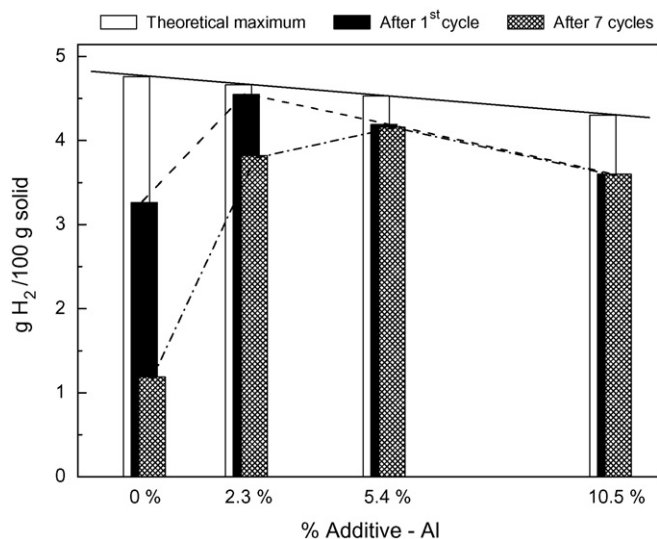


Fig. 5. Hydrogen storage density of Al added oxides.

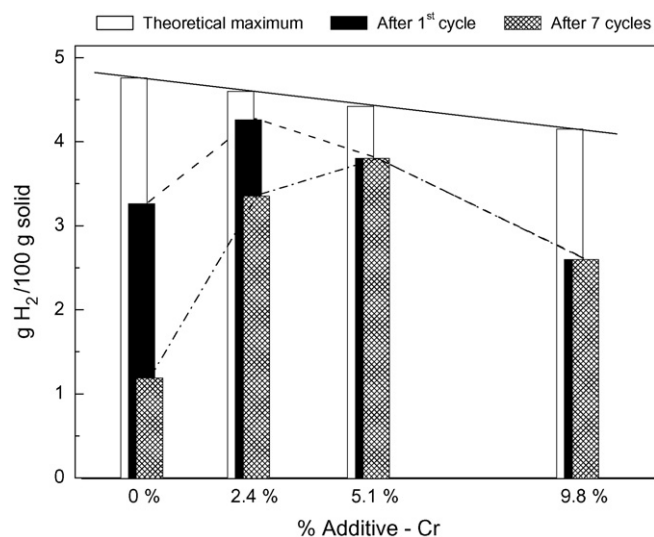


Fig. 6. Hydrogen storage density of Cr added oxides.

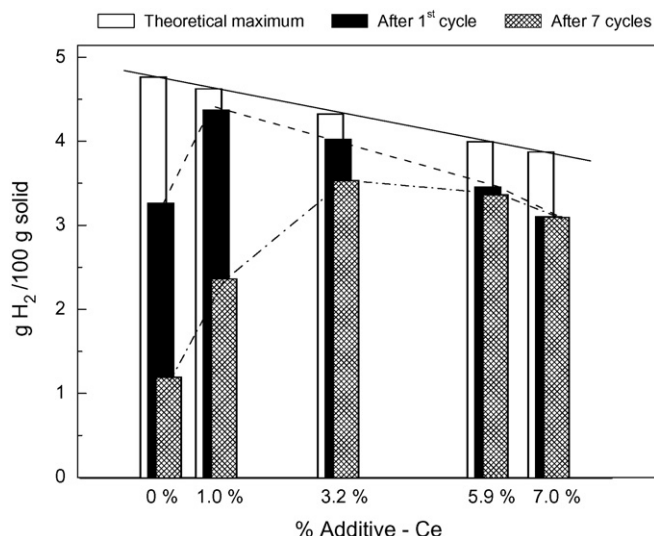


Fig. 7. Hydrogen storage density of Ce added oxides.

Finally, to facilitate the comparison between pure iron oxide and the iron oxides with additives, the results obtained when hematite was tested at the same experimental conditions are shown in all the cases.

Concerning Fig. 4 (mass changes of the iron based oxides with different amounts of additives, registered during the redox cycle experiments) and by examining the initial reduction step, it can be seen (as expected from the hydrogen TPR-TG tests) that the oxides with Al or Cr present lower reduction rates in comparison with the pure iron oxide. This fact is more remarkable for the samples with larger concentrations of Al or Cr, the times for which complete reduction is several times longer than that corresponding to the oxides with the lowest concentrations. For this reason, and in order to avoid too long experiments, the initial reduction step of the FeCr-10 iron oxide was performed at 500 °C (and thus the resulting reduction curve is not shown in Fig. 4b).

As it was shown in previous works [9], under the experimental conditions and the fixed oxidation length of the present study, the former oxide cannot be regenerated through iron oxidation with steam, but magnetite is obtained as the only product. Therefore, the initial reduction of the oxide and the reduction of the samples in subsequent cycles do not necessarily follow the same pattern, as can be seen in Fig. 4.

The successive reduction steps of the oxides with Al in subsequent cycles (Fig. 4a) show poorer kinetics than the oxide without additives. However, in this case, the differences due to the additive concentration are not as severe as they were in the first cycle. In contrast, from the second cycle on, the reduction rates of the oxides with any Cr content (Fig. 4b) are similar to the rates registered for the pure iron oxide, and therefore greater than the corresponding values exhibited by the oxides with Al. These observations denote that, except for the first reduction step, the iron oxide samples containing Cr had a similar behaviour to the iron oxide without additives. By analyzing the first reduction step for the oxides with Ce as additive (Fig. 4c), it can be seen that independently of the Ce content, the weight loss curves are very similar to each other and practically coincident with the pure iron oxide reduction curve. This result is consistent with the hydrogen TPR-TG tests and represents one of the main differences between the behaviour of the oxides with Ce and the previously studied additives (Al and Cr). In the same way, the improved reduction rates observed in the first step keep constant along the cycles.

On the other hand, regarding the oxidation process analogous results were obtained for the oxides with Al, Cr or Ce as additives. In all cases, these additives have a significantly favourable effect on the oxidation step, as compared with the behaviour of the pure iron oxide.

It can be seen that even for the lowest additive proportions, after the first oxidation, approximately 89% of the weight that is lost during the first reduction step, is regenerated. Assuming that the initial weight loss is due to the reduction of hematite to iron, a regeneration of 89% implies that the complete oxidation of Fe into magnetite is achieved.

The percentage of mass regenerated through the oxidation decreases gradually from the first to the seventh cycle for the iron oxides with lower concentrations of additive, whereas it keeps practically constant for the oxides with larger additive contents. These results verify that the incorporation of Al, Cr or Ce into the iron oxide extraordinarily enhances the stability of the solid, just as it was intended when they were selected as candidate additives.

The reasons of the favourable effect of these additives can be found in literature [16–18]. The presence of compound oxides of metal additives and iron was found by means of X-ray absorption near edge structure (XANES) and extended X-ray absorption fine structure (EXAFS) analysis. These compounds would inhibit the contact between iron metal particles, thus preventing the degra-

dation of the solids avoiding collapse of near grains. In addition to the resistance to sintering, the compound oxides present on the surface may activate the redox reactions.

On the other hand, by comparing the behaviour of the solids in terms of their hydrogen storage density (which is shown in Figs. 5–7), the following information may be inferred: the higher stability of the oxides with the larger additive content is reflected in the maintenance of the amount of hydrogen released after the first and seventh oxidations. However, although for these highly additivated oxides the corresponding curves of relative weight change (Fig. 4) indicated that nearly all the Fe previously formed was transformed into magnetite, the values of the hydrogen storage density (which were calculated from the experimental data) are lower than the maximum value, theoretically determined. This fact is especially true for the oxide with the higher content of additive and implies that, even though an apparent total stability is achieved, the activity of the stable oxide is lower than the theoretical maximum.

A possible explanation for this result is that, during the first reduction step, not all the iron oxide present in the sample was reduced, either because the time for reduction was not enough, or because part of the iron was in combination with the additive forming some stable compound, so that it was not able to reduce.

Regarding the oxides with the lowest additive percentage, their hydrogen storage density after the first redox cycle is higher compared to the rest of solids with the same additive. However, due to the decrease of activity of these oxides, after the seventh cycle, the hydrogen storage density (although still much higher compared to the iron oxide without additives) is always lower than the value obtained for the iron oxides with intermediates percentages of additive (around 5 mol%).

Consequently, it is clear that an optimum amount of additive exists for which the additivated oxide would lead to the maximum amount of hydrogen storage per weight of solid, virtually constant during all the redox cycles.

As main differences between the graphs in Figs. 5–7, it must be emphasized that, since the molecular weight of Cr is bigger than that of Al, the theoretical hydrogen storage density, calculated for the same percentage of additive, is lower for the oxide containing Cr (Fig. 6). For instance, the theoretical maximum amount of hydrogen that could be stored using a FeAl-10 iron oxide is 4.32%, whereas for a FeCr-10 oxide this value is calculated to be 4.14%. Furthermore, it can be observed that the discrepancy between the theoretical values of hydrogen storage density and the ones calculated from the experimental data is more remarkable in the FeCr case, especially for the oxide with the largest amount of Cr. This fact could be explained by taking into account that the iron oxides with Cr exhibited poor kinetics during the first reduction step.

Since Ce is the additive with the largest molecular weight of the three metals studied in this work, the incorporation of this additive into the iron oxides leads (Fig. 7) to the lowest hydrogen storage densities (as compared to the solids with Al and Cr, with the same additive content). It can be concluded that the hydrogen storage density of an oxide with a percentage of added Ce oxide is significantly lower than the analogous values of this parameter for oxides with the same concentration of Cr or Al oxides.

Similarly, it was proven that the experimentally calculated values of amount of hydrogen released (per mass of reduced solid) after seven cycles, by the iron oxides with a percentage of additive around 5 mol%, follow the same trend as shown by the theoretical values: 4.16%, 3.8% and 3.36% for the oxides with 5.4 mol% of Al, 5.1 mol% of Cr and 5.9 mol% of Ce, respectively.

It is interesting to mention these values, because with such amount of additive a repetitive regeneration of mass during the oxidations is achieved along seven cycles (apparent complete stability). Furthermore, among the studied oxides, the previously mentioned ones gave the maximum values of hydrogen storage density and therefore they can be considered nearly optimum values.

#### 4. Conclusions

The reduction and oxidation features of several iron oxides with various proportions of Al, Cr and Ce have been proven.

The behaviour during the initial hydrogen reduction step of the iron oxides with different amounts of Ce as additive was similar to the behaviour of the pure iron oxide. However, the iron oxides modified with Al and Cr exhibited poorer kinetics, this fact being more remarkable for increasing proportion of additives.

The addition of Al, Cr and Ce to the iron oxide greatly improved the stability and oxidation activity of the solids, during the repeated reduction–oxidation cycles.

For all cases, an optimum percentage of metal additive (around 5 mol%) could be found, for which the maximum amount of hydrogen storage density, practically constant along the cycles, was achieved.

#### Acknowledgements

The authors wish to acknowledge the financial support of DGI (Spain) for this work (CTQ2007-63420/PPQ) and the research grant AP2003-3632 hold by E. Lorente.

Also, financial aid for this study has been provided by CENIT SPHERA Project (CDTI Spain). Thanks must be given to Gas Natural S.A. (Spain), leader of this project.

#### References

- [1] V. Hacker, R. Fankhauser, G. Faleschini, H. Fuchs, K. Friedrich, M. Muhr, K. Korde-sch, *J. Power Sources* 86 (2000) 531–535.
- [2] M. Selan, J. Lehrhofer, K. Friedrich, K. Korde-sch, G. Simader, K. Otsuka, A. Mito, S. Takenaka, I. Yamanaka, *J. Power Sources* 61 (1996) 247–253.
- [3] P.B. Tarman, R. Biljetina, *Coal Process. Technol.* 5 (1979) 114–116.
- [4] <http://www.naturalhy.net>.
- [5] K. Otsuka, A. Mito, S. Takenaka, I. Yamanaka, *Int. J. Hydrogen Energy* 26 (2001) 191–194.
- [6] P. Gupta, L.G. Velazquez-Vargas, L.S. Fan, *Energy Fuels* 21 (2007) 2900–2908.
- [7] S. Fukase, T. Suzuka, *Appl. Catal. A: Gen.* 100 (1993) 1–17.
- [8] M. Thaler, V. Hacker, M. Anilkumar, J. Albering, J.O. Besenhard, H. Schröttner, M. Schmied, *Int. J. Hydrogen Energy* 31 (2006) 2025–2031.
- [9] E. Lorente, J.A. Peña, J. Herguido, *Int. J. Hydrogen Energy* 33 (2008) 615–626.
- [10] K. Otsuka, T. Kaburagi, C. Yamada, S. Takenaka, *J. Power Sources* 122 (2003) 111–121.
- [11] K. Otsuka, C. Yamada, T. Kaburagi, S. Takenaka, *Int. J. Hydrogen Energy* 28 (2003) 335–342.
- [12] S. Takenaka, N. Hanaizumi, V.T.D. Son, K. Otsuka, *J. Catal.* 228 (2004) 405–416.
- [13] S. Takenaka, K. Nomura, N. Hanaizumi, K. Otsuka, *Appl. Catal. A: Gen* 282 (2005) 333–341.
- [14] K. Urasaki, Y. Sekine, N. Tanimoto, E. Tamura, E. Kikuchi, M. Matsukata, *Chem. Lett.* 34 (2005) 230–231.
- [15] K. Urasaki, N. Tanimoto, T. Hayashi, Y. Sekine, E. Kikuchi, M. Matsukata, *Appl. Catal. A: Gen* 288 (2005) 143–148.
- [16] K. Otsuka, S. Takenaka, *J. Jpn. Petrol. Inst.* 47 (2004) 377–386.
- [17] S. Takenaka, T. Kaburagi, C. Yamada, K. Nomura, K. Otsuka, *J. Catal.* 228 (2004) 66–74.
- [18] V. Galvita, T. Hempel, H. Lorenz, L.K. Rihko-Struckmann, K. Sundmacher, *Ind. Eng. Chem. Res.* 47 (2008) 303–310.
- [19] P. Ciambelli, S. Cimino, G. Lasorella, L. Lisi, S. De Rossi, M. Faticanti, G. Minelli, P. Porta, *Appl. Catal. B: Environ.* 37 (2002) 231–241.
- [20] E. Lorente, Ph.D. Thesis, University of Zaragoza, 2008.
- [21] J.A. Peña, E. Lorente, E. Romero, J. Herguido, *Catal. Today* 116 (2006) 439–444.